Hindawi
Journal of Zoological Systematics and Evolutionary Research
Volume 2023, Article ID 3411188, 13 pages
https://doi.org/10.1155/2023/3411188

Research Article

Refining the "Melting Pot" Genus *Holosticha s. l.* (Protozoa, Ciliophora, Hypotrichia) Based on Multigene Datasets with Establishment of a New Species *Caudikeronopsis monilata* sp. nov.

Xumiao Chen,[1] **Ju Li**,[1,2] **and Kuidong Xu**[1,3]

[1]*Laboratory of Marine Organism Taxonomy and Phylogeny, Qingdao Key Laboratory of Marine Biodiversity and Conservation, Institute of Oceanology, Chinese Academy of Sciences, Qingdao 266071, China*
[2]*Qingdao Marine Product Museum, Qingdao 266003, China*
[3]*University of Chinese Academy of Sciences, Beijing 100049, China*

Correspondence should be addressed to Kuidong Xu; kxu@qdio.ac.cn

Received 3 January 2023; Revised 10 March 2023; Accepted 24 March 2023; Published 22 May 2023

Academic Editor: Miroslawa Dabert

The genus *Holosticha s. l.* is a typical "melting pot" group with an intricate history, and so far, it has been divided into eleven genera. Both newly obtained taxonomic and molecular data provide the opportunity to gain more insights to outline the taxa in it and to understand their systematic and evolutionary relationship. Here, we describe *Caudikeronopsis monilata* sp. nov. from intertidal sediment on the China coast of the Yellow Sea and analyze the phylogenetic relationships of *Holosticha s. l.* by obtaining a total of 16 new sequences of seven isolates. The results demonstrate that (1) the morphological features of *Holosticha s. str.* are outlined very well, but its systematic relationship with *Uncinata* is still puzzling; (2) based on both morphological and molecular databases, the genera *Adumbratosticha*, *Arcuseries*, *Caudikeronopsis*, *Extraholosticha*, and "*Holosticha* + *Uncinata*" complex are separated clearly from each other in the phylogenetic analyses; and (3) the *Anteholosticha* isolates are dispersed among the urostylids in the phylogenetic analyses, even though its generic diagnostic features are described very clearly. In the present work, however, the secondary structure predictions do not provide better resolutions for understanding the systematic and evolutionary relationships among the holostichids. And the genus *Anteholosticha* becomes a new "melting pot" taxon.

1. Introduction

As common members of the periphyton, benthos and psammon in marine, brackish, and freshwater habitats, the species-rich hypotrichous ciliates are much more diverse than previously thought, and their supraspecific categories and systematic relationship have been drawn more and more attention. *Holosticha* Wrzesniowski, 1877, has ever been a large and puzzling genus, in which over 100 species were originally assigned to it, and many others were transferred to and excluded from it [1–7]. With the continuous discovery of new taxa, the phylogenetic analyses based on multigene data provide the opportunity to break the *Holosticha s. l.* "melting pot," to gain more insights to outline to the taxa in it and to better understand their systematic and evolutionary relationship [8].

Caudikeronopsis was a monotypic genus established by Li et al. [5] with *C. marina* [9] as the type. In this study, we describe a new species of *Caudikeronopsis* from intertidal sediment on the China coast of the Yellow Sea. Based on reliable identification, we also newly obtain 16 sequences (five of SSU rDNA, six of ITS1-5.8S-ITS2, and five of LSU rDNA) of seven holostichid isolates including *Caudikeronopsis monilata* sp. nov. In order to infer the evolutionary relationships within the confusing holostichids, the phylogenetic analyses were conducted using these multiple markers and new sequences, and the secondary structure predictions

of SSU rRNA and ITS regions were also investigated. This paper attempts to improve our understanding of the diversity and phylogeny of hypotrichous ciliates through historical revision of the representative "melting pot" genus *Holosticha*.

2. Material and Methods

2.1. Ciliate Collection and Identification. Seven isolates of holostichids were collected from the coastal areas in Qingdao, China (Table 1), including the *Caudikeronopsis monilata* sp. nov., which was isolated from intertidal sediment in Qingdao Bay (36°03′39″N, 120°19′31″E), Qingdao, China, with salinity 30 psu and water temperature about 14°C. Living cells were maintained in the Petri dishes with habitat water at ambient temperature (ca. 20°C), and examined in vivo using a bright field and differential interference microscope at magnifications of 100-1000 ×. The infraciliature and nuclear structure were revealed using protargol impregnation according to Wilbert [10]. The species identification was achieved through both living observation and protargol staining based on raw culture.

2.2. DNA Extraction and Gene Sequencing. Specimens in the present work were isolated and washed using sterile marine water repeatedly. Genomic DNA extraction was conducted using DNeasy Blood & Tissue Kit (Qiagen, Hiden, Germany), according to the manufacturer's instructions. Using primers Primer A (5′-AACCTGGTTGATCCTGCCAGT-3′), Primer B (5′-TGATCCTTCTGCAGGTTCACCTAC-3′), ITS-F (5′-GTAGGTGAACCTGCGGAAGGATCATTA-3′) and R3 (5′-CATTCGGCAGGTGAGTTGTTACAC-3′), respectively, the PCR amplification for SSU rDNA, ITS1-5.8S-ITS2 and 5′ end of LSU rDNA sequences was conducted [11–13]. The amplification was following [14].

2.3. Phylogenetic Analyses. Using CLUSTAL W implemented in BioEdit 7.0 [15], the pairwise alignments of the sequences are conducted. The sites which are gaps in more than half of the sequences were excluded resulting in matrixes of 1785, 588, 1859, and 4158 characters for SSU rDNA, ITS1-5.8S-ITS2, LSU rDNA, and concatenated rDNA analyses, respectively. The pairwise distances between species/populations were calculated with MEGA 6.06 [16]. Modeltest 3.4 [17] and MrModeltest version 2.0 [18] were used for model selection of the maximum-likelihood (ML) and Bayesian inference (BI) analysis, respectively. According to the Akaike information criterion (AIC), the GTR+I+G model was selected as the optimal choice for SSU rDNA, LSU rDNA, and concatenated rDNA, and the GTR+G model was selected as the optimal choice for ITS1-5.8S-ITS2. The ML analyses were performed using RAxML-HPC2 on XSEDE 8.2.12 [19, 20] on the CIPRES Science Gateway (http://www.phylo.org/sub_sections/portal; [21]). With MrBayes 3.2.2 [22] via the CIPRES Science Gateway, Bayesian inference analyses were also conducted. The TreeView v1.6.6 [23] and MEGA 4.0 [24] were used to visualize tree topologies. The classification shown in the phylogenetic analyses is according to Berger [3], Huang et al. [4], and Luo et al. [6].

2.4. Topology Testing. PAUP was used to build eight unrooted trees with enforced topological constraints. The site-wise likelihoods for the best-unconstrained ML tree and all constrained trees were calculated in PAUP under the GTR+I+G model (for SSU rDNA, LSU rDNA, and concatenated rDNA) and GTR +G model (for ITS1-5.8S-ITS2) with parameters as suggested by Modeltest 3.4 [17]. The statistical probability of the constrained trees was evaluated in the likelihood frameworks through the approximately unbiased (AU) test [25], as implemented in the CONSEL software package [26].

2.5. Secondary Structure Predictions. The secondary structures of the variable regions 4 and 9 of SSU rRNA and ITS regions were computed by submission of primary sequences to the RNA folding website supporting MFOLD version 3.6 (http://unafold.rna.albany.edu/?q=mfold/RNA-Folding-Form; [27]), using the default parameters for folding except $T = 25 \circ$ C. The secondary structures of variable regions 4 and 9 of SSU rDNA were predicted based on the models of the eukaryotic SSU rRNA presented by Wuyts et al. [28] and Wang et al. [29]. The sequences of ITS regions were constrained according to the rules suggested by Yi et al. [13]. The structures were edited with RNA VIZ 2.0 [30] to produce acceptable illustrations.

3. Results

3.1. ZooBank Registration. Present work: SIDurn:lsid:zoobank.org:pub:78F09A0B-0BB0-457A-965D-214DDAEE1655. *Caudikeronopsis monilata* sp. nov.: urn:lsid:zoobank.org:act:F1E4D812-379D-4F96-AA1E-F2AD7BC50CF1.

3.2. Caudikeronopsis monilata sp. nov. (Figure 1)

3.2.1. Diagnosis. Marine *Caudikeronopsis* with the size 140 – 190 μm × 45 – 55 μm in vivo. Body ellipsoidal with length-to-width ratio about 3.4 : 1. Macronucleus in 3–6 nodules along the midline of the body and one to three micronuclei. Adoral zone comprising 35–65 membranelles; midventral complex composed of 11–16 cirral pairs extending to 4–8 transverse cirri; one left and one right marginal cirral row; two to four caudal cirri and 4–8 dorsal kineties.

3.2.2. Etymology. The Latin adjective *monilata* refers to the moniliform macronucleus of this species.

3.2.3. Type Locality. A sandy beach in Qingdao (36°03′39″N, 120°19′31″E), China, with a salinity of 30 psu and water temperature of about 14°C.

3.2.4. Material Deposited. The holotype slide (registration number: LJ14021502-1) and two paratype slides (LJ14021502-2 and LJ14021502-3) with protargol-impregnated specimens have been deposited in the Marine Biological Museum, Chinese Academy of Sciences, Qingdao. The holotype and paratype specimens are marked with black ink circles on the cover glass.

3.2.5. Description. Size 140 – 190 μm × 45 – 55 μm in vivo, the ratio of body length to width is about 3.4 : 1. Cell grey to grey-brown under low magnification, never contractile, with anterior end hyaline and slightly narrow and posterior

Table 1: Characterization of newly sequenced isolates investigated in this study.

Isolates	Collection site	Water temperature and salinity	Accession numbers		
			SSU rDNA	ITS1-5.8S-ITS2	LSU rDNA
Anteholosticha multicirrata	Qingdao Bay, Qingdao, China 36°03′39″N, 120°19′31″E	14°C, 30 psu	KX138645	KX099172	KX099170 KX099171
Anteholosticha pulchra	Qingdao Bay, Qingdao, China 36°03′39″N, 120°19′31″E	14°C, 33 psu	KX099173	/	/
Caudikeronopsis marina	Qingdao bay, Qingdao, China 36°03′39″N, 120°19′31″E	20°C, 27 psu	/	KX099175 KX099176	KX099174
Caudikeronopsis monilata sp. nov.	Qingdao Bay, Qingdao, China 36°03′39″N, 120°19′31″E	14°C, 30 psu	KX099177	KX099179	KX099178
Holosticha diademata	Qingdao Bay, Qingdao, China 36°03′39″N, 120°19′31″E	10°C, 30 psu	MT472015	/	/
Holosticha sp.	Qingdao port, Qingdao, China 36°05′17″N, 120°19′21″E	4°C, 33 psu	MT476978	MT476975	MT476979
Uncinata bradburyae	Qingdao port, Qingdao, China 36°05′17″N, 120°19′21″E	15°C, 33 psu	/	MT472616	/

end is broadly rounded. Dorsoventrally flattened ca. 4 : 3 (Figure 1, F). Macronucleus in 3–6 spherical nodules distributed along the midline of the body, recognizable in vivo, and each 7–14 μm in length after protargol impregnation (Figure 1, D (Ma)). One to three ellipsoidal micronuclei, about 5 μm × 8 μm after protargol impregnation (Figure 1, D (Mi)). Pellicles are thick and not easily deformed. Cortical granules are colorless, spherical, and size of about 3 μm × 2 μm; arranged among cirral rows on the ventral side and densely distributed on the dorsal side (Figure 1, B and K (arrows)). Cytoplasm grey, food vacuole 5–8 μm across and located posterior of body.

Locomotion by slow crawling on debris and sometimes static; thigmotactic and seldom bending, sometimes rotating around the longitudinal axis of the body when swimming.

Adoral zone of membranelles (AZM) question mark shaped, consisting of 35–65 membranelles and occupying about 30% of body length. Cilia in the apical part of AZM are about 19 μm long (Figure 1, K (arrowheads), and others are about 10μm long. Buccal cavity is narrow and flat, with the paroral membrane (PM) about half as long as the endoral membrane (EM).

Most cirri with cilia are about 11 μm in length except for transverse cirri with cilia about 20 μm long. One buccal cirrus locating at the right of the paroral membrane and single parabuccal cirrus is behind the rightmost frontal cirrus. Consistently two frontoterminal cirri located left of anterior right marginal cirral row. Invariably three enlarged frontal cirri connecting to the midventral complex composed of 11–16 cirral pairs. Four to eight transverse cirri adjacent to the posterior part of the midventral complex, with two pretransverse ventral cirri, one left and one right marginal cirral row with 30–58 and 34–54 cirri, respectively. Two to four caudal cirri and four to eight dorsal kineties with cilia about 7 μm long, conspicuous in vivo (Figure 1, J (arrows)).

3.3. SSU rDNA, ITS1-5.8S-ITS2, LSU-rDNA, and rDNA Topologies (Figures 2–5). A total of 16 sequences (five of SSU rDNA, six of ITS1-5.8S-ITS2, and five of LSU rDNA) of seven holostichid isolates, including *Caudikeronopsis monilata* sp. nov., were newly obtained. Their sampling information and accession numbers are provided in Table 1. Based on the molecular information available, the phylogenetic analyses have been expanded to 60 holostichid isolates belonging to seven genera, that is, *Adumbratosticha*, *Anteholosticha*, *Arcuseries*, *Caudikeronopsis*, *Extraholosticha*, *Holosticha*, and *Uncinata*.

The results showed that seven to 26 *Anteholosticha* isolates disperse in the urostylids. By contrast, the different isolates in both *Arcuseries* and *Caudikeronopsis* assemble very well with high support values, respectively (Figures 2, 4, and 5). In all the topologies, *Anteholosticha pulchra* nests, in the pseudokeronopsids, and *Anteholosticha gracilis* locate with *Monocoronella carnea* steadily.

For *Adumbratosticha* and *Extraholosticha*, there is only one specie that has molecular data. *Adumbratosticha tetracirrata* falls into the core urostylids based on SSU rDNA and ITS1-5.8S-ITS2 sequences (Figures 2 and 3). *Extraholosticha sylvatica* locates near to *Eschaneustyla lugeri* in SSU rDNA, LSU rDNA, and rDNA topologies (Figures 2, 4, and 5).

Uncinata isolates keep inside the *Holosticha* isolates, and they cluster together with high support values in all the topologies (Figures 2, 4, and 5), except for the phylogenetic trees based on ITS1-5.8S-ITS2 (Figure 3).

Except for the ITS1-5.8S-ITS2 trees, all the holostichid isolates form two main clades: *Adumbratosticha*, *Anteholosticha*, and *Extraholosticha* form one with the core urostylids, while *Arcuseries*, *Caudikeronopsis*, *Holosticha*, and *Uncinata* form the other one (Figures 2–5).

3.4. Topology Testing. The monophyly of the genus *Holosticha* is not rejected based on the ITS1-5.8S-ITS2 and LSU rDNA dataset but is rejected based on the SSU rDNA and rDNA datasets by the AU test. The statistical tests carried out on single gene do not reject the possibility of *Uncinata* and *Holosticha* forming a monophyletic clade.

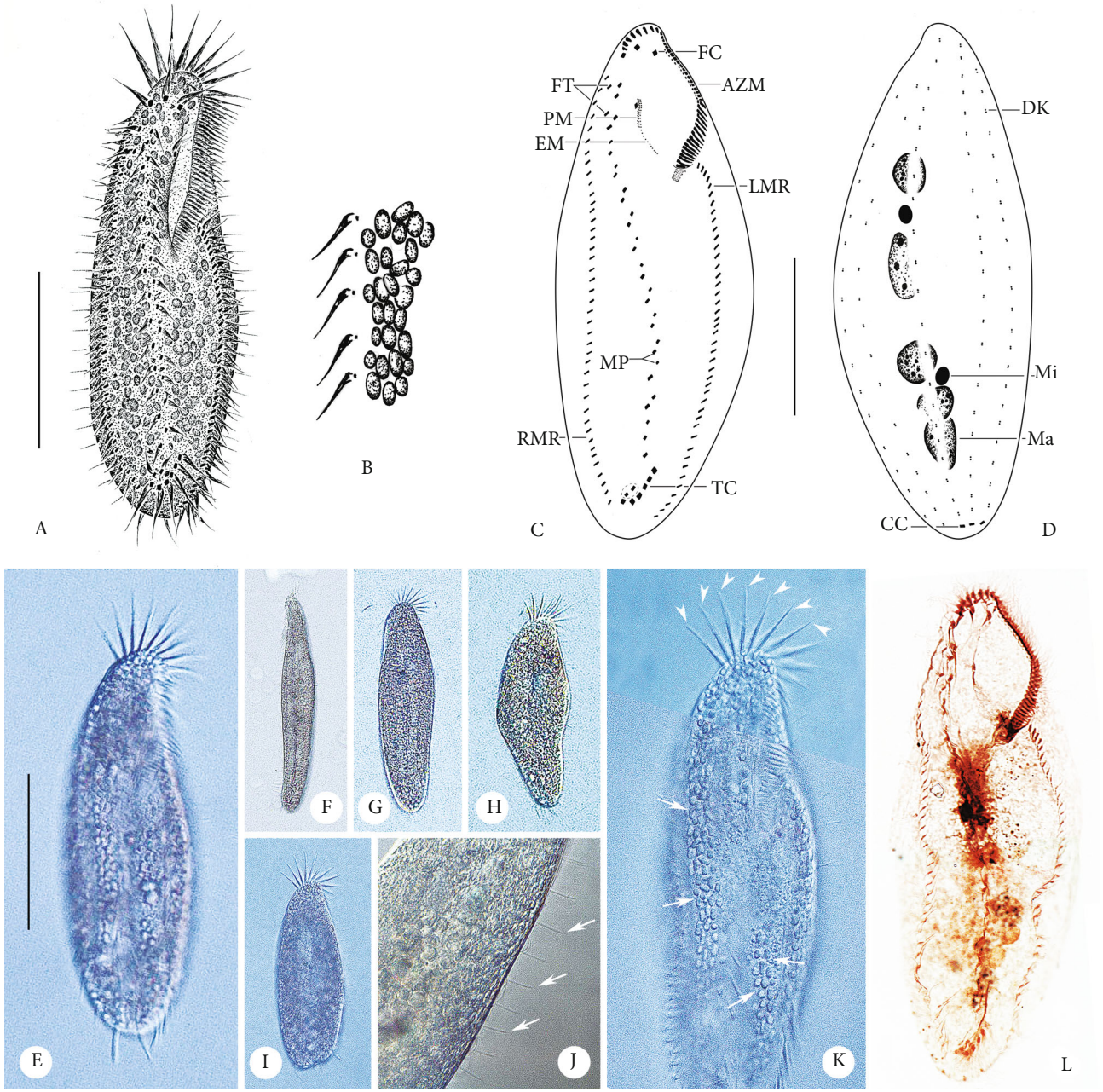

Figure 1: *Caudikeronopsis monilata* sp. nov. from life (A, B, E–K) and after protargol impregnation (C, D, L). (A, E) Ventral view of a representative specimen. (B) Cortical granules on the ventral side. (C, D, L) Ventral and dorsal view of the holotype indicating ciliary and nuclear pattern. (F–I) Body variations in lateral and ventral view. (J) Arrows marking dorsal kineties. (K) Ventral view to indicate adoral membranes (arrowheads) and cortical granules (arrows). AZM: adoral zone of membranelles; CC: caudal cirri; DK: dorsal kineties; EM: endoral membrane; FC: frontal cirri; FT: frontoterminal cirri; LMR: left marginal cirral row; Ma: macronuclear nodules; Mi: micronuclei; MP: midventral cirral pairs; PM: paroral membrane; RMR: right marginal cirral row; TC: transverse cirri. Scale bars = 60 μm.

3.5. Prediction and Comparison of the SSU rRNA Secondary Structures of V4 and V9 Regions (Figure 6). The partial putative secondary structures (helix E23-1/2 and helix E23-4/7) of the V4 regions of 58 holostichid isolates are investigated (Figure 6(a)). The structures of the V4 region are not conserved, that is, the number and position of bulges in helices E23-1/2 and E23-4/7 are not stable. The isolates in the genera *Arcuseries* and *Holosticha* have their own special motifs, respectively. There are many GC pairs in both the base part of helix E23-1/2 and around the middle bulge in helix E23-4/7 in the *Arcuseries* isolates. And some *Anteholosticha* isolates, the genus *Caudikeronopsis*, and *Extraholosticha sylvatica* isolates also have five to eight GC pairs in the base part of helix E23-1/2 (Figure 6(a), yellow markers). The

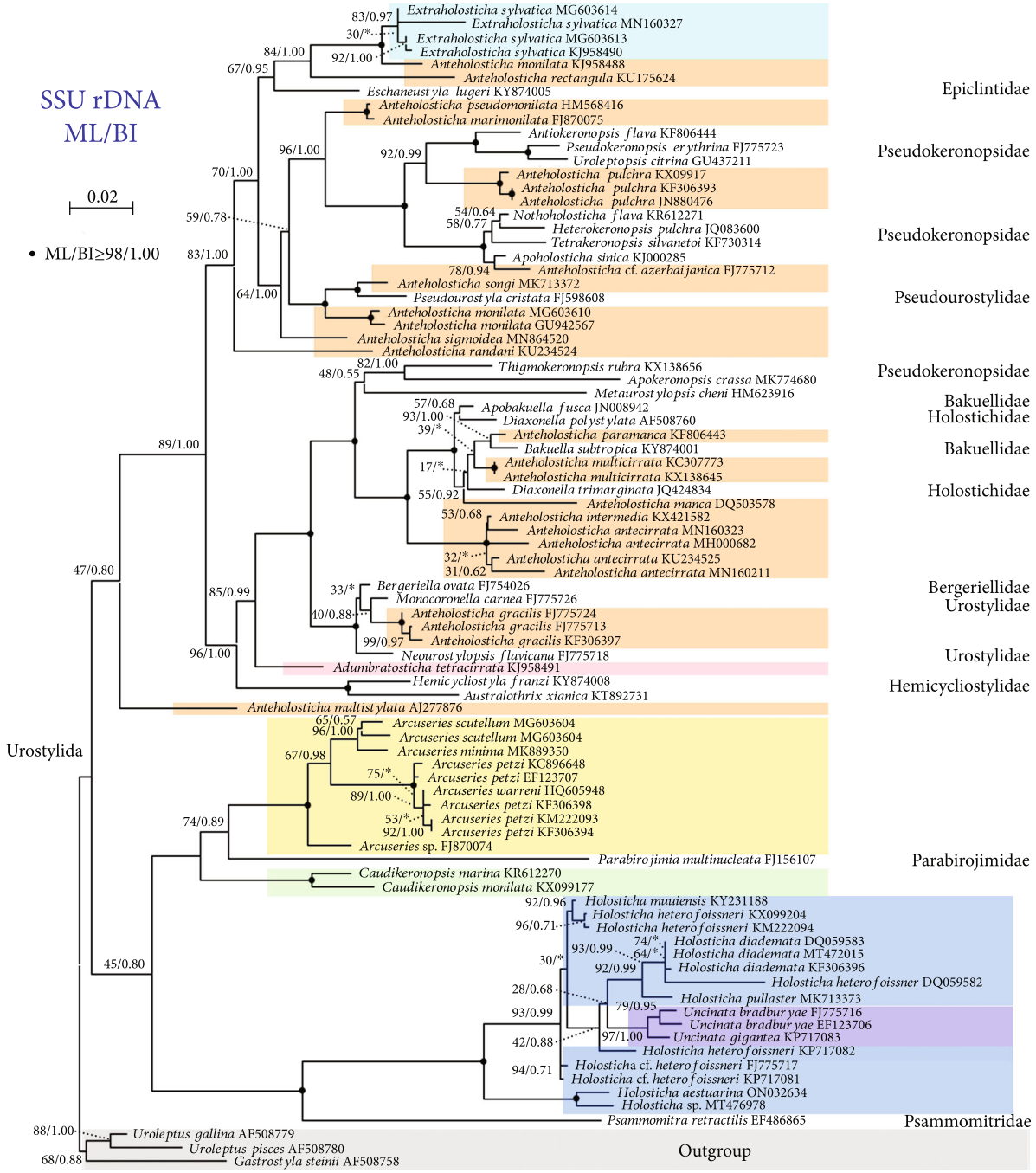

Figure 2: Maximum-likelihood (ML) and Bayesian inference (BI) phylogenetic trees based on SSU rDNA sequences showing the positions of holostichid isolates. Numbers near branches indicate the bootstrap values from ML and posterior probabilities of BI and the asterisk (*) indicates that the branch is not supported by BI phylogenetic trees. The scale bar corresponds to two substitutions per 100 nucleotide positions.

isolates in the genus *Holosticha* have the conserved motif 5′-UUGG versus CUGG-3′ near the terminal part in helix E23-4/7. And this feature also occurs in some *Anteholosticha* isolates, *Adumbratosticha tetracirrata*, the genus *Caudikeronopsis*, *Extraholosticha sylvatica* isolates, and the genus *Uncinata* (Figure 6(a), blue markers).

The partial putative secondary structures of the V9 regions of 44 holostichid isolates are investigated (Figure 6(b)). The structures of the V9 regions are much more conserved than those of the V4 region, that is, the number and position of bulges are stable. The motifs 5′-GAGUG versus CACUU-3′ and 5′-UU versus AA-3′ (Figure 6(b), grey markers) appear in all the 44 holostichid and many other urostylid. *Uncinata bradburyae* isolates have one UA-pair and one UG-pair astride the motif 5′-GAGUG versus CACUU-3′, beside which *Holosticha* isolates have one UA-pair or one UG-pair

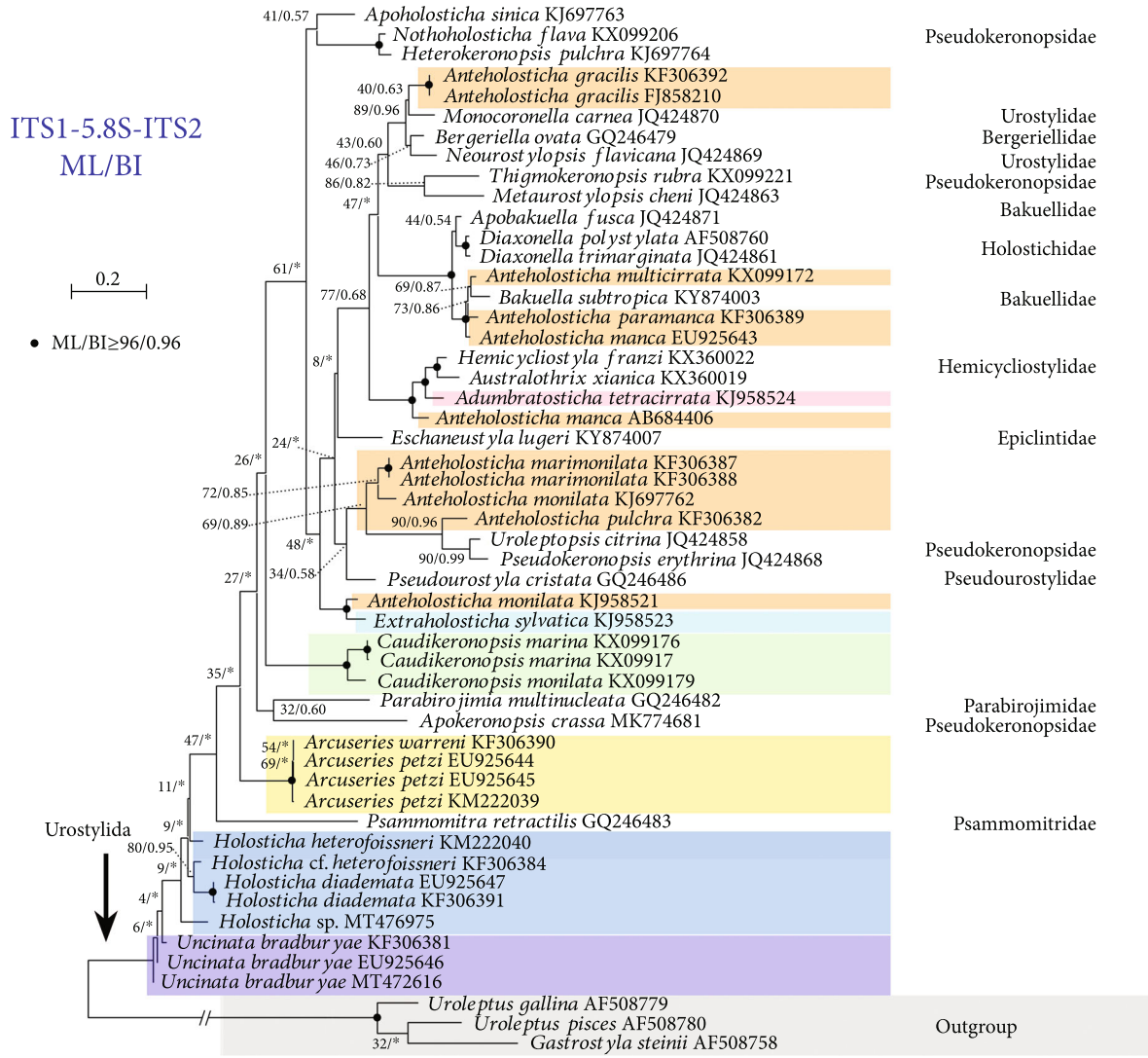

Figure 3: Maximum-likelihood (ML) and Bayesian inference (BI) phylogenetic trees based on ITS1-5.8S-ITS2 rDNA sequences showing the positions of holostichid isolates. Numbers near branches indicate the bootstrap values from ML and posterior probabilities of BI and the asterisk (*) indicates that the branch is not supported by BI phylogenetic trees. One long branch has been shortened as marked by "//," and the other branches are drawn to scale. The scale bar corresponds to twenty substitutions per 100 nucleotide positions.

(Figure 6(b), purple markers). Eight *Arcuseries* isolates have the motif 5′-GCGC versus GCGC-3′, which also appears in *Anteholosticha multistylata* and *Holosticha heterofoissneri* (Figure 6(b), yellow markers). The motifs 5′-CC versus GG-3′ and 5′-GG versus CC-3′ exist together in the three *Extraholosticha sylvatica* isolates and *Anteholosticha monilata* and present alone in several *Anteholosticha*, *Holosticha*, and *Uncinata bradburyae* isolates (Figure 6(b), green markers).

3.6. Putative Secondary Structures of ITS1 and ITS2 Transcripts (Figure 7). The putative structures of the ITS1 and ITS2 transcripts of the 27 and 28 holostichid isolates are predicted, and the general models based on these structures are proposed, respectively (Figure 7).

The ITS1 has three helices, which exhibit distinct size classes. As the most conserved one, helix I comprise only UA pairs in most holostichid isolates. As special cases, helix I in *Caudikeronopsis* isolates is the motifs 5′-CUC versus GAG-3′ (Figure 7(a), green markers); and there is an unpaired CC (Figure 7(a), purple markers) among the UA pairs in helix I of *Uncinata bradburyae* isolates. Helix II is special and variable, which can separate the genera *Arcuseries*, *Caudikeronopsis*, *Holosticha*, and *Uncinata* clearly from other holostichid isolates. Helix II in *Arcuseries* isolates is 48 nt and has fifteen GC pairs (Figure 7(a), yellow markers). *Caudikeronopsis* isolates have the motifs 5′-GUGC versus GCGC-3′ and 5′-GC versus GC-3′ in the middle and at the terminal end of Helix II, respectively. These two motifs are also present in some other holostichid isolates together or partly (Figure 7(a), green markers). Helix II in *Holosticha* and *Uncinata* isolates both have the motifs 5′-GCG versus CGC-3′ (Figure 7(a), purple markers) and 5′-GUGC versus

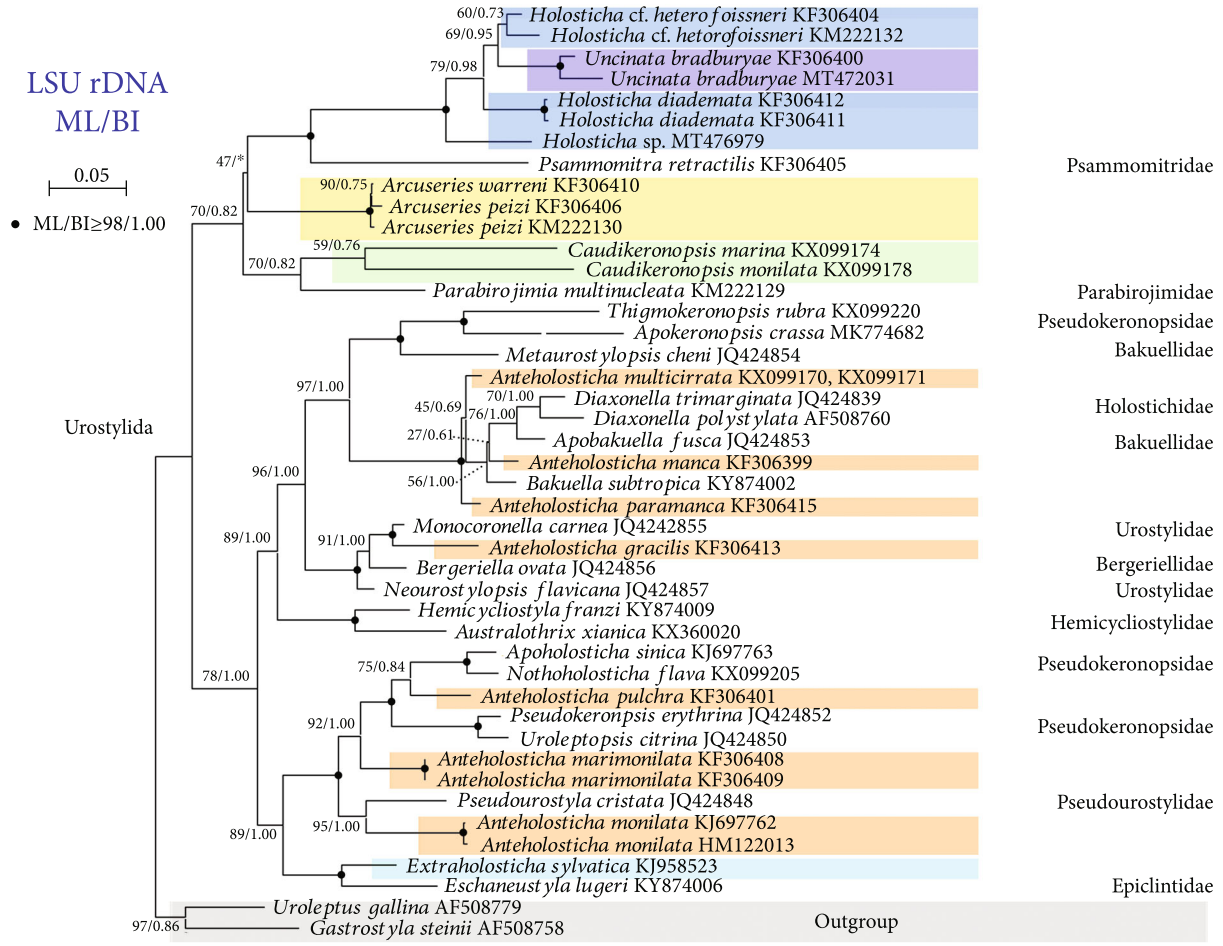

FIGURE 4: Maximum-likelihood (ML) and Bayesian inference (BI) phylogenetic trees based on LSU rDNA sequences showing the positions of holostichid isolates. Numbers near branches indicate the bootstrap values from ML and posterior probabilities of BI and the asterisk (*) indicates that the branch is not supported by BI phylogenetic trees. The scale bar corresponds to five substitutions per 100 nucleotide positions.

GCGC-3′ at the base and in the middle of helix II, respectively. Helix III can separate *Holosticha* and *Uncinata* isolates from other holostichid isolates, with the motifs 5′-UAAA versus UUUA-3′ and 5′-CU versus AG-3′ at the base and terminal end (Figure 7(a), blue markers), which only two *Anteholosticha* species have.

There are two helices in ITS2, that is, helix A 10-16 nt long and helix B 72-112 nt long. In helix A, all the holostichid isolates have the motif 5′-GA/GGA versus UCUC-3′ near the terminal loop. Except for *Caudikeronopsis*, all the other holostichid isolates have three branches in the helix B, in which the right one has the same motif 5′-CA/GG versus CUG-3′ (Figure 7(b), orange markers). All the holostichid isolates are very similar to each other in the middle branch (Figure 7(b), grey markers). *Caudikeronopsis* isolates have the motifs 5′-GCCUCUGC versus GU/CAGAGGU/C and 5′-GCGGG versus CCCGC-3′ in helix B (Figure 7(b), green markers), and the first one also occurs in *Adumbratosticha tetracirrata*, some *Holosticha*, and *Uncinata bradburyae* isolates. *Holosticha* isolates have the motif 5′-AAG versus CUU-3′ at the base of helix B, which some other holostichid isolates also have (Figure 7(b), blue markers).

4. Discussion

4.1. Morphological Comparison of Caudikeronopsis monilata sp. nov. with Related Taxa. Li et al. [5] established the monotypic genus *Caudikeronopsis* for *C. marina*, which was originally reported as *Caudiholosticha marina* by Li et al. [9]. Our isolate accords with the diagnostic features of *Caudikeronopsis* very well. Compared to the type species *C. marina*, *C. monilata* sp. nov. has a smaller body size (140–190 μm vs. 210–310 μm in vivo), a much smaller number of midventral pairs (11–16 vs. 23–37) as well as macronuclear nodules (3–6 vs. 10–20) [9].

4.2. Historical Revision of the Genus Holosticha (Figure 8). *Holosticha* Wrzesniowski, 1877, was a large genus, in which more than 100 species were originally described. Berger [2] recognized 49 species of *Holosticha s. l.*, assigned only seven species to the genus *Holosticha s. str.*, and established three

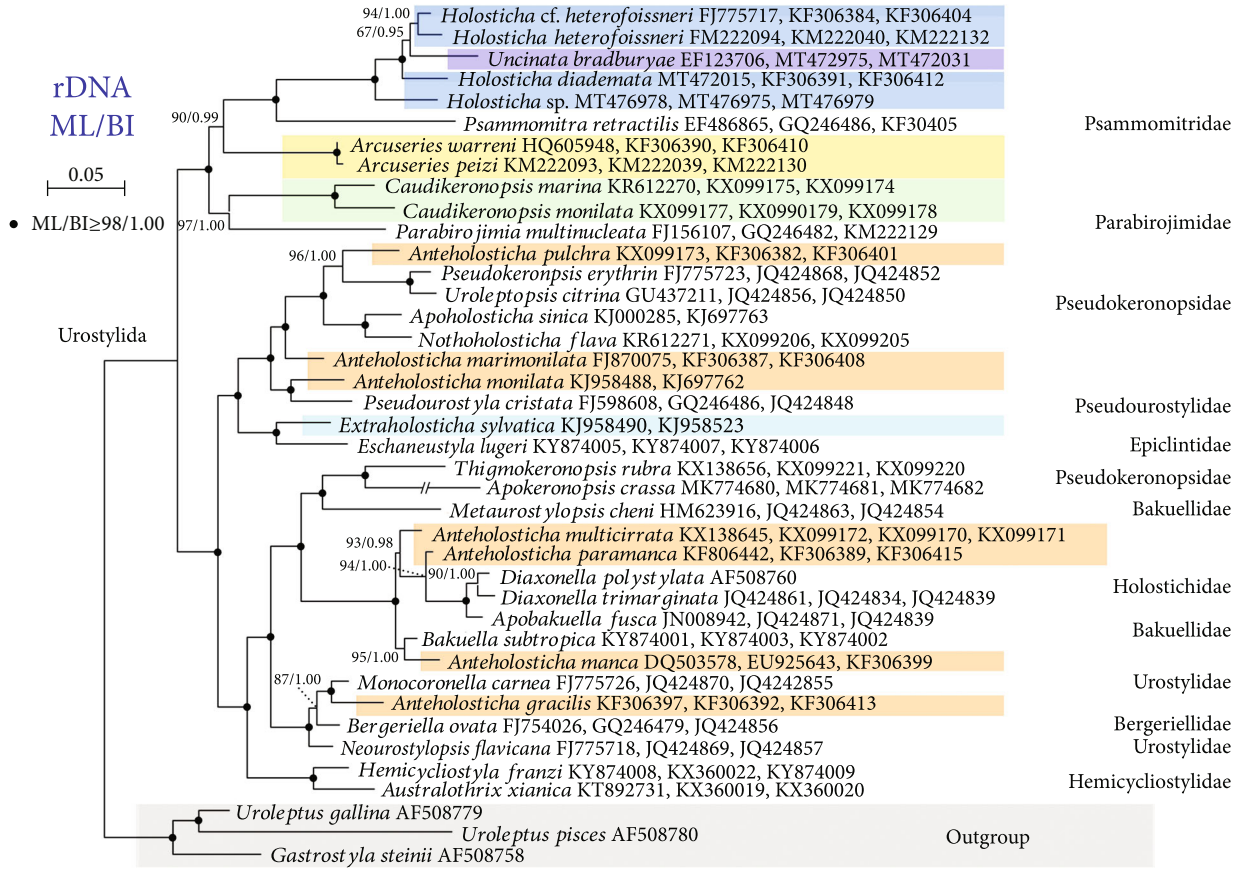

Figure 5: Maximum-likelihood (ML) and Bayesian inference (BI) phylogenetic trees based on rDNA sequences showing the positions of holostichid isolates. Numbers near branches indicate the bootstrap values from ML and posterior probabilities of BI and the asterisk (*) indicates that the branch is not supported by BI phylogenetic trees. The scale bar corresponds to five substitutions per 100 nucleotide positions.

genera *Anteholosticha* [2], *Caudiholosticha* [2], and *Biholosticha* [2] to include the other species.

Since molecular phylogeny largely focused on limited sampling, the incongruence between morphological data and gene sequences has been arising. By collecting the three-gene data (SSU rDNA, ITS1-5.8S-ITS2, and LSU rDNA) comprising 30 species in the "core urostyloids," Huang et al. [4] established *Arcuseries* containing three distinctly deviating *Anteholosticha* species, with the character of roughly U-shaped arranged transverse cirri (Figure 8, yellow arrow).

Combining the morphological, morphogenetic, and SSU rDNA-based phylogenetic analyses, Luo et al. [6] transferred *Holosticha bradburyae* Gong et al., 2001 to *Uncinata*, due to its possession of a characteristically prominent beak-like, leftwards curved projection and the developmental mode of the dorsal kineties (Figure 8, purple arrows).

Berger [2] established *Caudiholosticha* with *Holosticha stueberi* Foissner, 1987 as type, and, a total of 17 species have been classified in it till 2016 [3, 9, 31]. Li et al. [5] confirmed that the type species of *Caudiholosticha* should not belong to the urostyloids, but to the nonoxytrichid dorsomarginalian genus *Uroleptus* Ehrenberg, 1831 because of its dorsomarginal kineties. Hence, the other 16 species lacking dorsomarginal kineties, were reclassified to six newly established urostyloid genera: *Acuholosticha*, *Adumbratosticha*, *Caudikeronopsis*, *Extraholosticha*, *Limnoholosticha*, and *Multiholosticha* [5]. And their infraciliature patterns are indicated in the grey box in Figure 8.

However, due to a lack of detailed information on the ciliary pattern, morphogenetic process and molecular data, the taxonomy and systematics of *Limnoholosticha viridis* (Kahl, 1932) [5] were poorly known. Based on a Chinese population of this uncertain species, Song et al. [8] established a new genus *Bourlandella* for it. Considering its dorsal ciliature shares features (presence of dorsomarginal kinety and dorsal kinety 3 fragmentation) that are typical of oxytrichids, *Bourlandella* [8] might be an intermediate form between urostylids and dorsomarginalians.

4.3. Is Holosticha Outlined Well? After over decades' modification (Figure 2), the genus *Holosticha s. str.* is morphologically defined by a combination of features, that is, adoral zone of membranelles bipartite and rearmost ones wider, buccal cirrus distinctly ahead of paroral, number of transverse cirri nearly number of midventral pairs, anterior end of left marginal row composed of narrowly spaced cirri and distinctly curved rightwards, caudal cirri lacking [2]. Luo et al. [6] transferred *Holosticha bradburyae* (Gong et al. 2001) to *Uncinata*, due to its possession of a

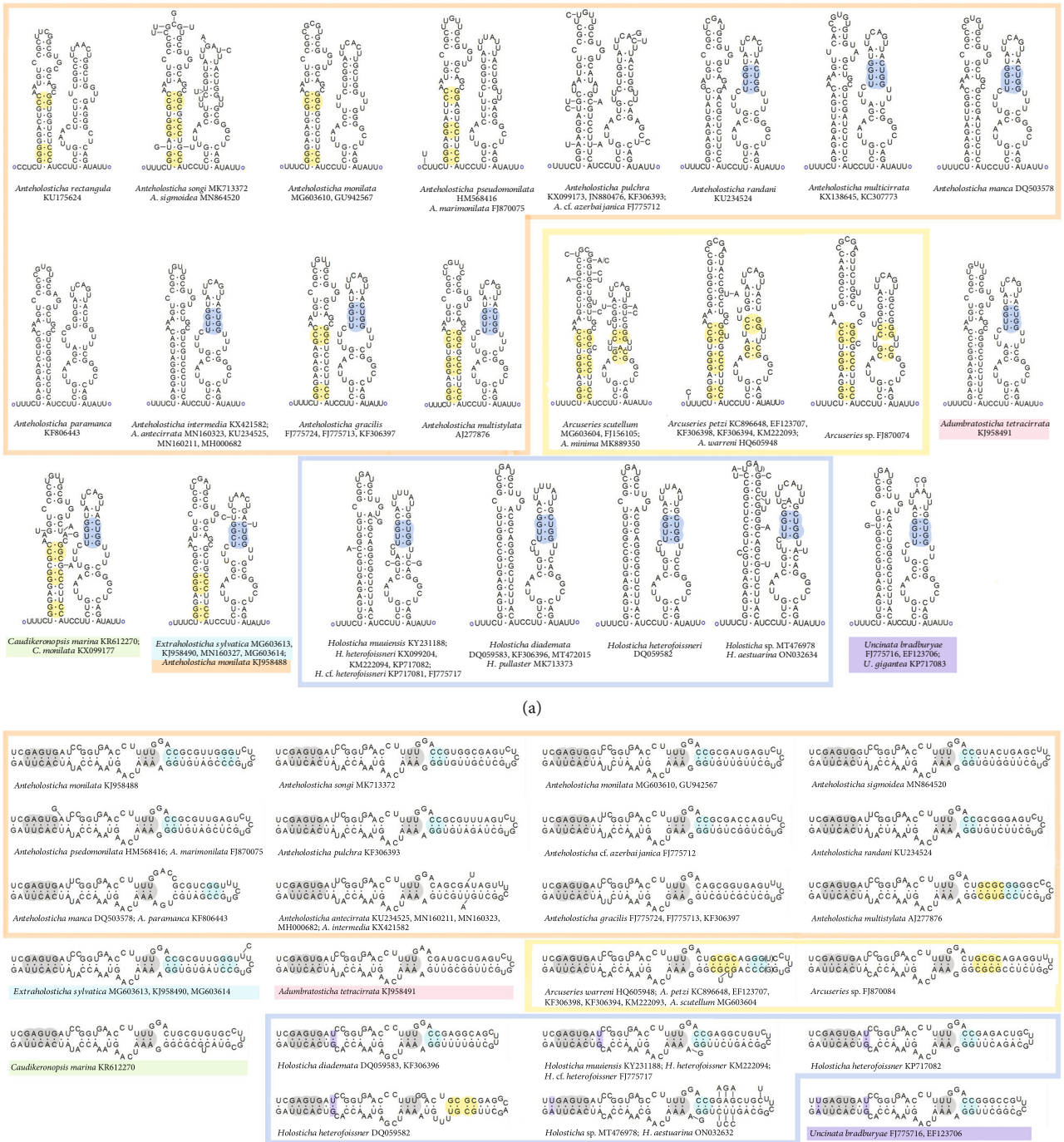

FIGURE 6: (a) Partial putative secondary structures of variable region 4 of the SSU rRNA comprising helices E23-1/2 and E23-4/7 for 59 holostichid isolates. (b) Partial putative secondary structures of variable region 9 of the SSU rRNA for 45 holostichid isolates.

characteristically prominent beak-like, leftwards curved projection and the developmental mode of the dorsal kineties. And the phylogenetic analyses revealed *Holosticha* to be monophyletic and sister to *Uncinata* [6].

However, the phylogenetic analyses by Zhang et al. [7] indicated that *Uncinata* is a subgenus of *Holosticha*. And in the present work, by adding new sequences of *Holosticha* sp. (MT476978 for SSU rDNA, MT476975 for ITS1-5.8S-ITS2 regions, and MT476979 for LSU rDNA), not only *Uncinata* isolates always nest in *Holosticha* isolates in the phylogenetic tree but also the monophyly of the genus *Holosticha* is not supported well. The genera *Holosticha* and *Uncinata* have a very close relationship, and their putative secondary structures of V4 and V9 in SSU rRNA, ITS1 and ITS2 share similar motifs with each other. Even though the possibility of *Uncinata* and *Holosticha* forming a

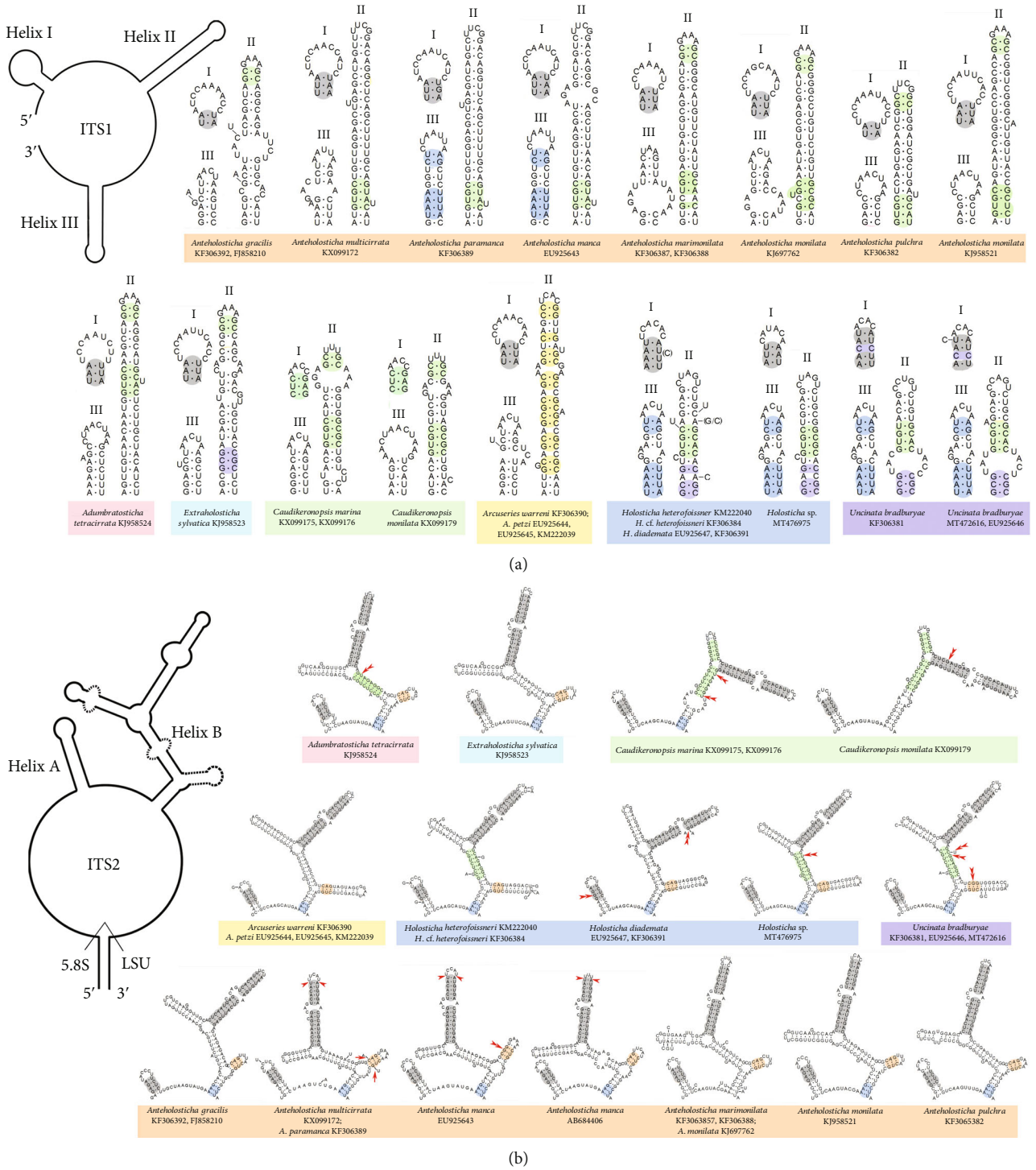

FIGURE 7: (a) The putative secondary model and structures of the ITS1 transcript in 28 holostichid isolates. (b) The putative secondary model and structures of the ITS2 transcript in 29 holostichid isolates. Arrows and double-arrowheads indicate the CBCs (compensatory base change) and hemi-CBCs, respectively. Arrowheads mark the sites lacking one pair of the compensatory base.

monophyletic clade is not all rejected, we cannot confirm that *Uncinata* isolates belong to the genus *Holosticha*.

Up to now, the morphological features of *Holosticha* and *Uncinata* are both outlined very well, but their systematic relationship with *Uncinata* is still puzzling. At least for a while, it is better to regard them as two separated genera.

4.4. Is Antholosticha a New "Melting Pot" Genus? Because of its intricate history, *Holosticha* had been a typical "melting pot" genus for many years until recently, most holostichid isolates divide into eleven genera (Figure 8). Based on both morphological and molecular databases, the genera *Adumbratosticha*, *Arcuseries*, *Caudikeronopsis*, *Extraholosticha*,

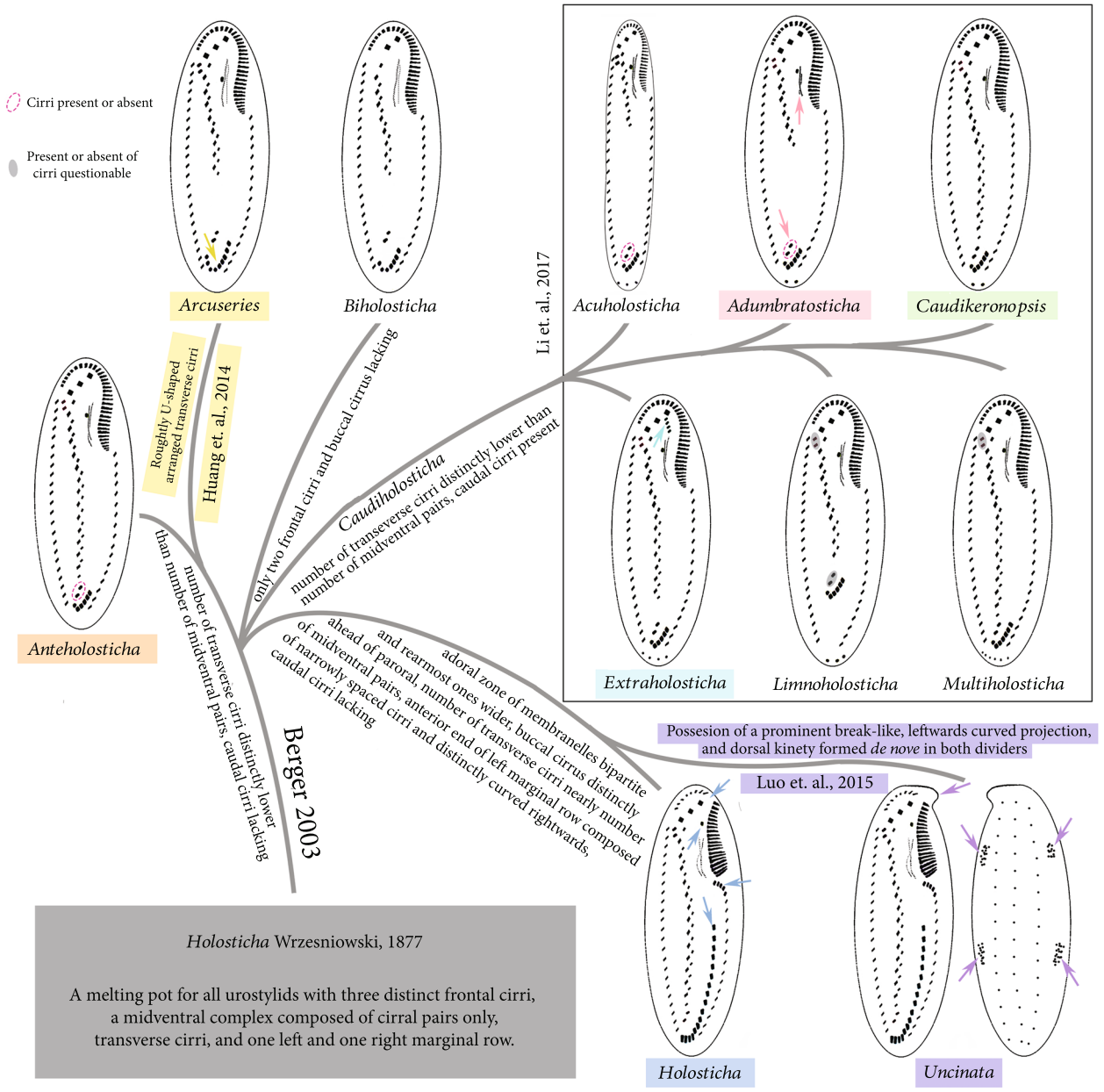

FIGURE 8: The historical revision of the holostichid isolates moved out of the "melting pot" genus *Holosticha*. Arrows indicate the diagnostic characters of different genera.

and "*Holosticha+Uncinata*" complex are outlined quite well, and they are separated clearly from each other in the phylogenetic analyses. In contrast, the genus *Anteholosticha* isolates disperse among the urostylids in the phylogenetic analyses, even though its morphologically diagnostic features are described very clearly. To a certain extent, *Anteholosticha* is now a new "melting pot" genus.

4.5. Do Secondary Structure Predictions Always Provide Better Resolutions for Phylogenetic Analyses? By predicting the secondary structures of four variable regions (V2, V4, V7, and V9) in the SSU rRNA of 45 urostylids, Wang et al. [29] considered the V4 region as the most effective in revealing interspecific relationships, while V9 appeared suitable at the family level or higher; V2 was too conserved to reflect phylogenetic relationships at the family or lower lever, and V7 was the least informative. Hence, in the present work, we focus on the relatively conserved E23-1/2 and E23-4/7 parts of the V4 region and V9 region. Both the shapes and conserved motifs of the V4 and V9 of SSU rRNA correspond well with the phylogenetic trees' topology with a visual manner.

With relatively high divergence, the secondary structure predictions of the internal transcribed spacer (ITS) regions are widely used for phylogenetic reconstructions below the family level [14, 32–35]. Among the holostichid isolates, the general secondary structure models are relatively stable,

and there are some compensatory base changes (CBCs) to maintain their reliability. Although less stable than the Watson-Crick complementarities, the GU appositions often occur in their ITS2 regions.

In the present work, however, the secondary structure predictions do not provide better resolutions for understanding the systematic and evolutionary relationships among the holostichids, as did in previous studies [14, 32]. The genus *Anteholosticha* becomes a new "melting pot," which is still puzzling.

Data Availability

The holotype slide (registration number: LJ14021502-1) and two paratype slides (LJ14021502-2 and LJ14021502-3) with protargol-impregnated specimens have been deposited in the Marine Biological Museum, Chinese Academy of Sciences, Qingdao. The holotype and paratype specimens are marked with black ink circles on the cover glass. The new sequences of SSU rDNA, ITS1-5.8S-ITS2, and LSU rDNA that support the findings of this study have been deposited in NCBI GenBank (Table 1). The registration of *Caudikeronopsis monilata* sp. nov. and the publication of the present work in ZooBank are as follows: urn:lsid:zoobank.org:act:F1E4D812-379D-4F96-AA1E-F2AD7BC50CF1 and LSID:urn:lsid:zoobank.org:pub:78F09A0B-0BB0-457A-965D-214DDAEE1655, respectively.

Conflicts of Interest

The authors declare that they have no conflicts of interest.

Acknowledgments

This work was supported by the National Natural Science Foundation of China (32270471 and 41876171).

References

[1] H. Berger, *Catalogue of Ciliate Names: Hypotrichs*, Verlag Helmut Berger, Salzburg, 2001.

[2] H. Berger, "Redefinition of *Holosticha* Wrzesniowski, 1877 (Ciliophora, Hypotricha)," *European Journal of Protistology*, vol. 39, no. 4, pp. 373–379, 2003.

[3] H. Berger, "Morphology, biology, and terminology," in *Monograph of the Urostyloidea (Ciliophora, Hypotricha)*, vol. 85 of Monographiae Biologicae, pp. 1–71, Springer, Dordrecht, 2006.

[4] J. Huang, Z. Chen, W. Song, and H. Berger, "Three-gene based phylogeny of the Urostyloidea (Protista, Ciliophora, Hypotricha), with notes on classification of some core taxa," *Molecular Phylogenetics and Evolution*, vol. 70, pp. 337–347, 2014.

[5] F. Li, Z. Lyn, Y. Li et al., "Morphology, morphogenesis, and molecular phylogeny of *Uroleptus* (*Caudiholosticha*) *stueberi* (Foissner, 1987) comb. nov. (Ciliophora, Hypotricha), and reclassification of the remaining *Caudiholosticha* species," *European Journal of Protistology*, vol. 59, pp. 82–98, 2017.

[6] X. Luo, F. Gao, K. A. S. Al-Rasheid, A. Warren, X. Hu, and W. Song, "Redefinition of the hypotrichous ciliateUncinata, with descriptions of the morphology and phylogeny of three urostylids (Protista, Ciliophora)," *Systematics and Biodiversity*, vol. 13, no. 5, pp. 455–471, 2015.

[7] Z. Zhang, H. Berger, H. Pan, and J. Jiang, "Two hypotrichs (Ciliophora, Hypotricha) from China: morphology and SSU rDNA sequence of *Holosticha aestuarina* nov. spec. and *H. muuiensis* Kim et al., 2017," *European Journal of Protistology*, vol. 86, article 125931, 2022.

[8] W. Song, T. Zhang, X. Zhang et al., "Taxonomy, ontogenesis and evolutionary relationships of the algae-bearing ciliate *Bourlandella viridis* (Kahl, 1932) comb. nov., with establishment of a new genus and new family (Protista, Ciliophora, Hypotrichia)," *Frontiers in Microbiology*, vol. 11, article 560915, 2021.

[9] J. Li, X. Chen, and K. Xu, "Morphology and small subunit rDNA phylogeny of two new marine urostylid ciliates, *Caudiholosticha marina* sp. nov. and *Nothoholosticha flava* sp. nov. (Ciliophora, Hypotrichia)," *Journal of Eukaryotic Microbiology*, vol. 63, no. 4, pp. 460–470, 2016.

[10] N. Wilbert, "Eine verbesserte technik der protargolimprägnation für ciliaten," *Mikrokosmos*, vol. 64, pp. 171–179, 1975.

[11] J. Gong, S. J. Kim, S. Y. Kim et al., "Taxonomic redescriptions of two ciliates, *Protogastrostyla pulchra* n. g., n. comb. and *Hemigastrostyla enigmatica* (*Ciliophora*: *Spirotrichea*, *Stichotrichia*), with phylogenetic analyses based on 18S and 28S rRNA gene sequences," *Journal of Eukaryotic Microbiology*, vol. 54, no. 6, pp. 468–478, 2007.

[12] L. Medlin, H. J. Elwood, S. Stickel, and M. L. Sogin, "The characterization of enzymatically amplified eukaryotic 16S-like rRNA- coding regions," *Gene*, vol. 71, no. 2, pp. 491–499, 1988.

[13] Z. Yi, X. Lin, A. Warren, K. A. S. Al-Rasheid, and W. Song, "Molecular phylogeny of *Nothoholosticha* (Protozoa, Ciliophora, Urostylida) and systematic relationships of the *Holosticha-complex*," *Systematics and Biodiversity*, vol. 8, no. 1, pp. 149–155, 2010.

[14] X. Chen, J. Li, and K. Xu, "Insights into the phylogeny of three systematically controversial subfamilies of urostylid ciliates based on rDNA," *Zoologica Scripta*, vol. 50, no. 3, pp. 383–395, 2021.

[15] T. A. Hall, "BioEdit: a user-friendly biological sequence alignment editor and analysis program for windows 95/98/NT," *Nucleic Acids Symposium Series*, vol. 41, pp. 95–98, 1999.

[16] K. Tamura, G. Stecher, D. Peterson, A. Filipski, and S. Kumar, "MEGA6: molecular evolutionary genetics analysis version 6.0," *Molecular Biology and Evolution*, vol. 30, no. 12, pp. 2725–2729, 2013.

[17] D. Posada and K. A. Crandall, "Modeltest: testing the model of DNA substation," *Bioinformatics*, vol. 14, pp. 817-818, 1988.

[18] J. A. A. Nylander, *MrModeltest Version 2*, Department of Systematic Zoology, Evolutionary Biology Centre, Uppsala University, Uppsala, Sweden, 2004.

[19] A. Stamatakis, "RAxML-VI-HPC: maximum likelihood-based phylogenetic analyses with thousands of taxa and mixed models," *Bioinformatics*, vol. 22, no. 21, pp. 2688–2690, 2006.

[20] A. Stamatakis, P. Hoover, and J. Rougemont, "A rapid Bootstrap algorithm for the RAxML web servers," *Systematic Biology*, vol. 57, no. 5, pp. 758–771, 2008.

[21] M. A. Miller, W. Pfeiffer, and T. Schwartz, "Creating the CIPRES science gateway for inference of large phylogenetic trees," in *2010 Gateway Computing Environments Workshop (GCE)*, pp. 1–8, New Orleans, LA, USA, 2010.

[22] F. Ronquist and J. Huelsenbeck, "MRBAYES 3: Bayesian phylogenetic inference under mixed models," *Bioinformatics*, vol. 19, no. 12, pp. 1572–1574, 2003.

[23] R. D. M. Page, "TreeView: an application to display phylogenetic trees on personal computers," *Computer Applications in the Biosciences*, vol. 12, no. 4, pp. 357-358, 1996.

[24] K. Tamura, J. Dudley, M. Nei, and S. Kumar, "MEGA4: molecular evolutionary genetics analysis (MEGA) software version 4.0," *Molecular Biology and Evolution*, vol. 24, no. 8, pp. 1596–1599, 2007.

[25] H. Shimodaira, "An approximately unbiased test of phylogenetic tree selection," *Systematic Biology*, vol. 51, no. 3, pp. 492–508, 2002.

[26] H. Shimodaira and M. Hasegawa, "Consel: for assessing the confidence of phylogenetic tree selection," *Bioinformatics*, vol. 17, no. 12, pp. 1246-1247, 2001.

[27] M. Zuker, "Mfold web server for nucleic acid folding and hybridization prediction," *Nucleic Acids Research*, vol. 31, no. 13, pp. 3406–3415, 2003.

[28] J. Wuyts, R. D. Rijk, Y. V. Peer, G. Pison, P. Rousseeuw, and R. D. Wachter, "Comparative analysis of more than 3000 sequences reveals the existence of two pseudoknots in area V4 of eukaryotic small subunit ribosomal RNA," *Nucleic Acids Research*, vol. 28, no. 23, pp. 4698–4708, 2000.

[29] P. Wang, F. Gao, J. Huang, M. Strüder-Kypke, and Z. Yi, "A case study to estimate the applicability of secondary structures of SSU-rRNA gene in taxonomy and phylogenetic analyses of ciliates," *Zoologica Scripta*, vol. 44, no. 5, pp. 574–585, 2015.

[30] P. D. Rijk and R. D. Wachter, "RnaViz, a program for the visualisation of RNA secondary structure," *Nucleic Acids Research*, vol. 25, no. 22, pp. 4679–4684, 1997.

[31] W. Foissner, *Terrestrial and semiterrestrial ciliates (protozoa, Ciliophora) from Venezuela and Galápagos*, vol. 35, Denisia, 2016.

[32] X. Chen, J. Li, and K. Xu, "Multigene-based phylogeny analyses of the controversial family Condylostomatidae (Ciliophora, Heterotrichea)," *Zoologica Scripta*, vol. 49, no. 2, pp. 250–264, 2020.

[33] J. Li, W. Liu, S. Gao, A. Warren, and W. Song, "Multigene-based analyses of the phylogenetic evolution of oligotrich ciliates, with consideration of the internal transcribed spacer 2 secondary structure of three systematically ambiguous genera," *Eukaryotic Cell*, vol. 12, no. 3, pp. 430–437, 2013.

[34] M. Miao, A. Warren, W. Song, S. Wang, H. Shang, and Z. Chen, "Analysis of the internal transcribed spacer 2 (ITS2) region of scuticociliates and related taxa (Ciliophora, Oligohymenophorea) to infer their evolution and phylogeny," *Protist*, vol. 159, no. 4, pp. 519–533, 2008.

[35] P. Sun, J. C. Clamp, and D. Xu, "Analysis of the secondary structure of ITS transcripts in peritrich ciliates (Ciliophora, Oligohymenophorea): implications for structural evolution and phylogenetic reconstruction," *Molecular Phylogenetics and Evolution*, vol. 56, no. 1, pp. 242–251, 2010.